

## Few-group Cross-section Generation by Monte Carlo Code MCS for LWRs

Tung D. C. Nguyen, Setiawan Fathurrahman, Deokjung Lee\*

Ulsan National Institute of Science and Technology (UNIST), 50 UNIST-gil, Ulsan 44919, Republic of Korea

\*Corresponding author: deokjung@unist.ac.kr

### 1. Introduction

This paper represents the current status of the Monte Carlo (MC) code MCS, which has been developed from scratch at the Ulsan National Institute of Science and Technology since 2013 [1]. Its objectives include resolving computational reactor physics issues and developing a high-fidelity light water reactor (LWR) core simulation tool. Lately, the coupling of the MC and nodal diffusion codes to analyze reactors has aroused interest because of a solid motivation to initiate a sequence that could produce accurate solutions with reduced computational and time requirements. As a result, a recent MCS feature has been developed to generate the homogeneous assembly few-group cross-section (XS) for reactor core analysis using the conventional two-step procedure with the downstream nodal diffusion code, PARCS [2]. A verification against 2D APR1400 core benchmark problems [3] is conducted by MCS/PARCS two-step sequence and MCS as the reference solutions.

### 2. Methods and features

#### 2.1. Few-group XS generation

MCS must prepare the few-group XS before running the nodal diffusion code. To obtain the neutron flux spectrum, MCS first solves the neutron transport equation using the continuous energy XS library. The few-group XS [4] is then condensed utilizing calculated flux as the weighting function as in Eq. (1)

$$\Sigma_{x,g} = \frac{\int_V dV \int_{E_g}^{E_{g-1}} dE \Sigma_x(r, E) \phi(r, E)}{\int_V dV \int_{E_g}^{E_{g-1}} dE \phi(r, E)}, \quad (1)$$

where  $\phi(r, E)$  is the space-energy-dependent flux,  $V$  is the volume,  $g$  is the group index with upper and lower energy boundaries of  $E_g$  and  $E_{g-1}$ , and  $\Sigma_x(r, E)$  is a space-energy-dependent XS. XS type  $x$  would be  $t$  (total),  $tr$  (transport),  $f$  (fission), and  $a$  (absorption). The P0 and P1 scattering matrices are similarly spatially homogenized.

Furthermore, as shown in Eq. (2), the outflow transport correction method [4] has been widely used in lattice physics codes to approximate the transport XS. The inflow transport correction method is impractical

because the MC method could not precisely calculate the flux moment.

$$\Sigma_{tr,g} = \Sigma_{t,g} - \sum_{g'} \Sigma_{s,g' \rightarrow g}^1. \quad (2)$$

The B1 method is a common computational method for calculating the critical spectrum. MCS tallies the intermediate multi-group XS, which are then condensed into few-group XS (usually two groups) by using B1-leakage corrected critical spectra as a weighting function [5]. The following are the multi-group B1 equations:

$$\begin{cases} \Sigma_{t,g} \phi_g \pm iB J_g = \chi_g + \sum_{g'} \Sigma_{s,g' \rightarrow g}^0 \phi_{g'} \\ 3a_g(B) \Sigma_{t,g} J_g \pm iB \phi_g = 3 \sum_{g'} \Sigma_{s,g' \rightarrow g}^1 J_{g'} \end{cases}, \quad (3)$$

where  $\phi_g$  and  $J_g$  correspond to the neutron flux and current,  $B$  is the energy-independent buckling,  $\chi_g$  is the fission spectrum,  $\Sigma_{s,g' \rightarrow g}^0$  and  $\Sigma_{s,g' \rightarrow g}^1$  are, respectively, the P0 and P1 scattering matrices, and  $a_g(B)$  are defined as follows:

$$a_g(B) = \begin{cases} \frac{1}{3} x^2 \left( \frac{\arctan(x)}{x - \arctan(x)} \right), \\ \text{for } x^2 = \left( \frac{B/\Sigma_{t,g}}{\Sigma_{t,g}} \right)^2 > 0 \\ \frac{1}{3} x^2 \left( \frac{\ln\left(\frac{1+x}{1-x}\right)}{\ln\left(\frac{1+x}{1-x}\right) - 2x} \right), \\ \text{for } x^2 = -\left( \frac{B/\Sigma_{t,g}}{\Sigma_{t,g}} \right)^2 > 0 \end{cases}. \quad (4)$$

In the B1 method, the buckling search to make the assembly critical is done iteratively by adjusting the buckling until the multiplication factor equals one. The definition of multiplication factor is  $k_{\text{eff}} = \sum_g \nu \Sigma_{f,g} \phi_g$  where  $\nu$  is the number of neutrons released per fission. The solution of the B1 equation is to generate the diffusion coefficients as follows:

$$D_g = \frac{iJ_g}{|B| \phi_g}, \quad (5)$$

where  $D_g$  is the diffusion coefficient of group  $g$ . Then, condensing from intermediate multi-group to a few-

group diffusion coefficient is done using the critical spectrum.

## 2.2. Assembly discontinuity factor

In order to attain coupling between adjacent nodes in nodal codes, continuity conditions for neutron current and heterogeneous flux must be satisfied. As a result, the assembly discontinuity factor (ADF) [6] must be introduced to correct the discontinuous homogeneous flux at the node boundaries. The following is the definition of ADFs:

$$F_{g,k} = \frac{\phi_{s,g,k}^{hete}}{\phi_{s,g,k}^{homo}} = \frac{\frac{1}{S_k} \int_{S_k} d^2r \int_{E_g}^{E_{g-1}} dE \phi(r, E)}{\frac{1}{S_k} \int_{S_k} d^2r \Phi_g(r)}, \quad (6)$$

where  $\phi$  is the heterogeneous flux,  $\Phi$  is the homogeneous flux, and calculating the integration is over the boundary surface  $k$ .

The surface-averaged homogeneous flux equals the volume-averaged heterogeneous flux when the lattice calculation is run with reflective boundary conditions (BCs). Eq. (6) then becomes:

$$F_{g,k} = \frac{\phi_{s,g,k}^{hete}}{\phi_g^{hete}} = \frac{\frac{1}{S_k} \int_{S_k} d^2r \int_{E_g}^{E_{g-1}} dE \phi(r, E)}{\frac{1}{V} \int_V d^3r \int_{E_g}^{E_{g-1}} dE \phi(r, E)}. \quad (7)$$

The ADFs, in particular, can be calculated directly from the MC simulation. However, this is no longer the case if the BC is not reflective, i.e., the fuel assembly (FA) facing reflectors. As a result, an additional diffusion solver based on the analytical solution (analytic nodal method - ANM) corresponding to specified BCs is required to calculate the homogeneous surface flux at boundaries.

## 3. Numerical results

To verify the MCS/PARCS code sequence, the 2D APR1400 core benchmark problem is selected. The radial core configuration is depicted in Fig. 1. The APR1400 core contains 241 FAs arranged in a rectangular lattice. The typical geometry of the APR1400 FA, which contains 236 fuel or burnable absorber rods, four guide tubes, and one central tube, is depicted in Fig. 2. More information on the benchmark can be found in [3].

This paper adopts two benchmark problems corresponding to hot-zero power (HZP), and hot-full power (HFP) with a boron concentration of 1,000 ppm in

the moderator. The MCS standalone calculation (including the multiplication factor  $k_{eff}$  and power profiles) is used to verify the MCS/PARCS results. The ENDF/B-VII.1 library is used in all simulations. The following is the MC criticality set for the steady-state calculation to produce the reference solutions: 50 active batches, 5 inactive batches, 400 cycles per batch, and 20,000 histories per cycle are all possible. MCS calculates the assembly power with an average standard deviation of less than 0.25% and a maximum standard deviation of less than 1.5%, where the local fission power is low.

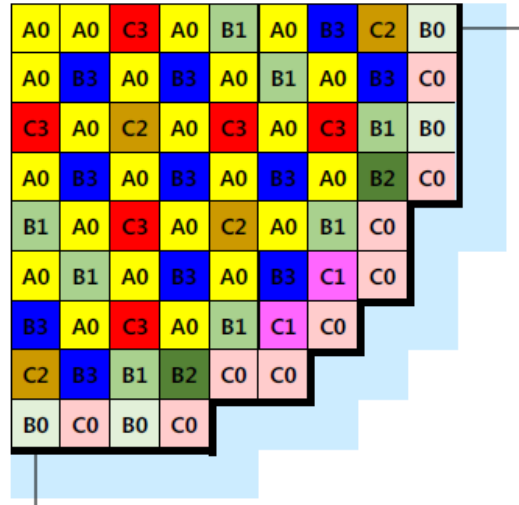


Fig. 1. APR1400 core configuration.

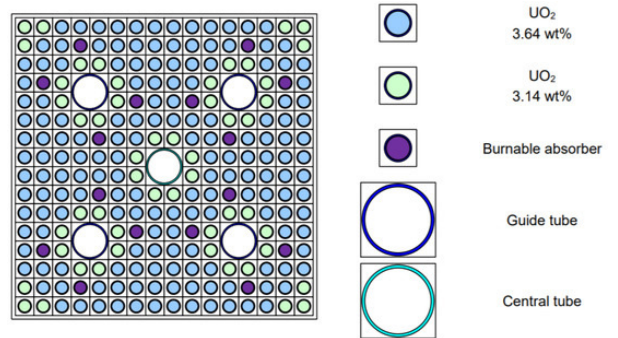


Fig. 2. Layout of C2 FA.

The simplified computation scheme for coarse mesh whole-core calculation with two-step code MCS/PARCS is shown in Fig. 3. MCS first generates the 2-group XSs and ADFs (group constants) for each assembly type using reflective BCs, with a 70-group intermediate group structure for solving the B1 equation. MCS employs the fuel-reflector model (as shown in Fig. 4) to obtain the fuel and reflector group constants in the case of FA adjacent to the reflector node. All surfaces in this model have reflective BC except the East one, which has vacuum BC. Finally, PARCS uses the generated group constants to calculate nodal diffusion.

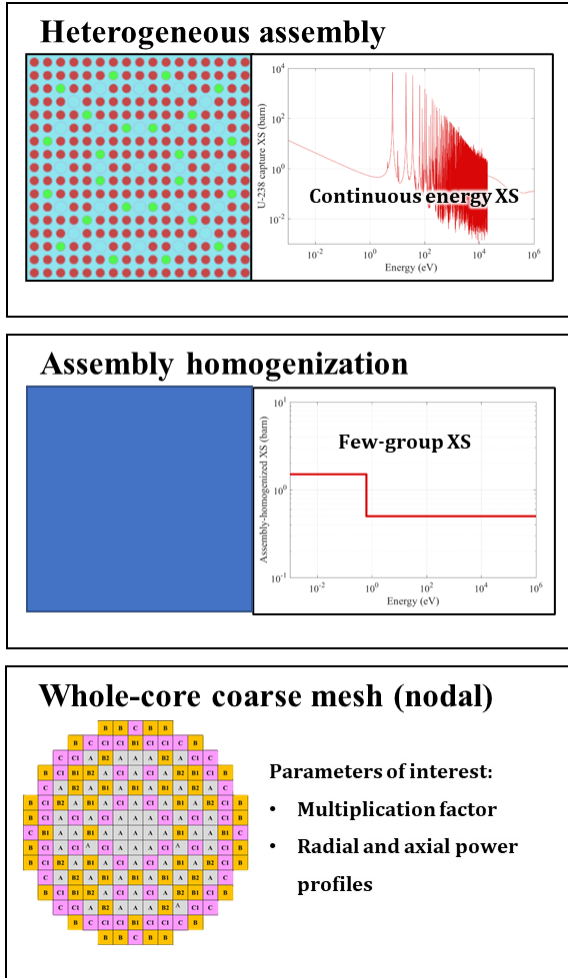


Fig. 3. Simplified computation scheme for coarse-mesh whole-core calculation.

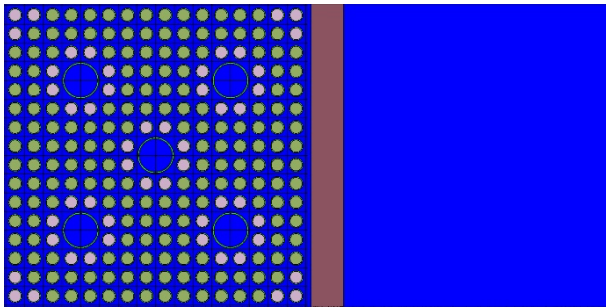


Fig. 4. Fuel-reflector model.

The comparison of the multiplication factor  $k_{eff}$  between MCS/PARCS and MCS is summarized in Table I. MCS/PARCS underestimates the  $k_{eff}$  by less than 100 pcm for HZP and HFP. A reasonable agreement indicates that 2-group B1 XS combined with ADFs can well preserve the reactivity of the MC solutions. To attain this statement, MCS/PARCS should add additional benchmarks, such as the 3D core case and control rod worth calculation.

Table I:  $k_{eff}$  comparison, MCS/PARCS vs. MCS

Case	MCS ( $\pm 4$ pcm)	MCS/PARCS	Diff. (pcm)
HZP	1.02262	1.02165	-93
HFP	1.01489	1.01413	-73

Figures 5-6 illustrate the MCS/PARCS radial assembly power distributions in octan geometry and a comparison to MCS. MCS/PARCS power distributions are primarily consistent with MCS reference solutions. In the case of HZP and HFP, the root-mean-square (RMS) error is less than 1.0 percent, and the maximum error is less than 2.2 percent. Choi et al. [5] found that using the outflow correction method significantly overestimates neutron leakage, resulting in an underestimate of the core multiplication factor in the presence of significant neutron leakage. Choi et al. [5] also prove that obtaining the critical spectrum using the P1 or CASMO-4E methods can improve the power profile predicted by the transport/nodal diffusion two-step code. Future work will involve incorporating those methods into MCS and determining the most promising combination to improve accuracy.

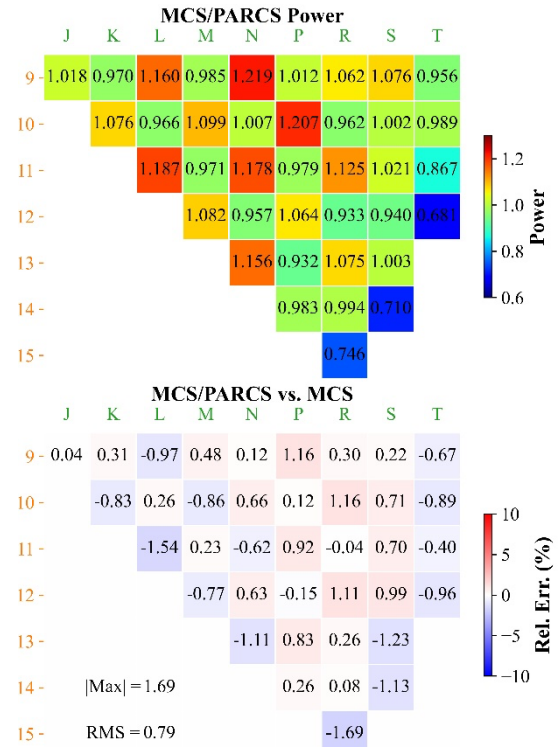


Fig. 5. MCS/PARCS assembly power and comparison to MCS at HZP.

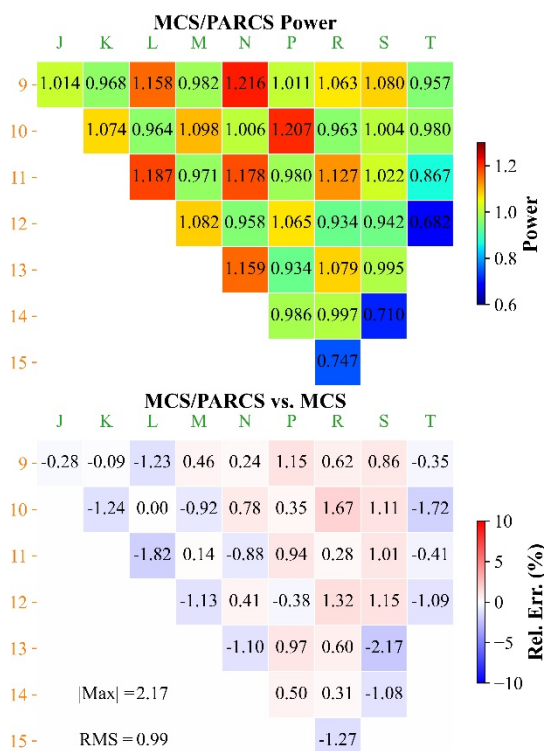


Fig. 6. MCS/PARCS assembly power and comparison to MCS at HFP.

#### 4. Conclusions

The feasibility of using the MCS MC code to generate few-group XSs and ADFs for LWR analysis using the nodal diffusion simulator, PARCS, is investigated in this paper. The 2D APR1400 core benchmark problems are used to validate the MCS/PARCS coupling code system. MCS generated the group constants, which included 2-group XS and ADFs, so that PARCS could predict the core  $k_{\text{eff}}$  and power profiles. A code-to-code comparison reveals reasonable agreement between MCS/PARCS and MCS results; the  $k_{\text{eff}}$  bias is less than 100 pcm, and the RMS differences in assembly power are less than 1.0% for HZP and HFP. Overall, when compared to the MC results, the B1 method with outflow correction demonstrated moderate accuracy due to fortunate error cancelation. To reduce the power error, more comprehensive features in MCS, such as using the P1 or CASMO-4E methods to calculate the critical spectrum, must be implemented.

#### Acknowledgments

This work was supported by the National Research Foundation of Korea (NRF) grant funded by the Korea government (MSIT). (No. NRF-2019M2D2A1A03058371).

#### REFERENCES

[1] Lee, H., Kim, W., Zhang, P., Lemaire, M., Khassenov, A., Yu, J., Jo, Y., Park, J. and Lee, D., 2020. MCS—A Monte Carlo particle transport code for large-

scale power reactor analysis. *Annals of Nuclear Energy*, 139, p.107276.

[2] Pirouzmand, A. and Mohammadhasani, F., 2016. PARCS code multi-group neutron diffusion constants generation using the Monte Carlo method. *Progress in Nuclear Energy*, 86, pp.71-79.

[3] Barr, K.E., Choi, S., Kang, J. and Kochunas, B., 2021. Verification of MPACT for the APR1400 Benchmark. *Energies*, 14(13), p.3831.

[4] Fridman, E. and Leppänen, J., 2011. On the use of the Serpent Monte Carlo code for few-group cross section generation. *Annals of Nuclear Energy*, 38(6), pp.1399-1405.

[5] Choi, S., Smith, K.S., Kim, H., Tak, T. and Lee, D., 2017. On the diffusion coefficient calculation in two-step light water reactor core analysis. *Journal of Nuclear Science and Technology*, 54(6), pp.705-715.

[6] Leppänen, J., Pusa, M. and Fridman, E., 2016. Overview of methodology for spatial homogenization in the Serpent 2 Monte Carlo code. *Annals of Nuclear Energy*, 96, pp.126-136.